P53 and Pten control neural and glioma stem/progenitor cell renewal and differentiation

Citation

Zheng, H., H. Ying, H. Yan, A. C. Kimmelman, D. J. Hiller, A. Chen, S. R. Perry, et al. 2014. "P53 and Pten control neural and glioma stem/progenitor cell renewal and differentiation." Nature 455 (7216): 1129-1133. doi:10.1038/nature07443. http://dx.doi.org/10.1038/nature07443.

Published Version

doi:10.1038/nature07443

Permanent link

http://nrs.harvard.edu/urn-3:HUL.InstRepos:12406668

Terms of Use

Share Your Story

The Harvard community has made this article openly available.
Please share how this access benefits you. Submit a story.

Accessibility

P53 and Pten control neural and glioma stem/progenitor cell renewal and differentiation

Hongwu Zheng[1,12], **Haoqiang Ying**[1,12], **Haiyan Yan**[1], **Alec C. Kimmelman**[1,2], **David J. Hiller**[6], **An-Jou Chen**[1], **Samuel R. Perry**[1,5], **Giovanni Tonon**[1], **Gerald C. Chu**[1,3,5], **Zhihu Ding**[1], **Jayne M. Stommel**[1], **Katherine L. Dunn**[1], **Ruprecht Wiedemeyer**[1], **Mingjian J. You**[1], **Cameron Brennan**[9,10], **Y. Alan Wang**[1,5], **Keith L. Ligon**[1,3,4,8], **Wing H. Wong**[6], **Lynda Chin**[1,5,7], and **Ronald A. DePinho**[1,5,11]

[1]Department of Medical Oncology, Harvard Medical School, Boston, MA

[2]Harvard Radiation Oncology Program, Harvard Medical School, Boston, MA

[3]Department of Pathology, Harvard Medical School, Boston, MA

[4]Division of Neuropathology, Harvard Medical School, Boston, MA

[5]Center for Applied Cancer Science, Belfer Foundation Institute for Innovative Cancer Science, Harvard Medical School, Boston, MA

[6]Department of Statistics, Stanford University, Stanford, CA

[7]Department of Dermatology, Brigham and Women's Hospital, Harvard Medical School, Boston, MA

[8]Center for Molecular Oncologic Pathology, Dana-Farber Cancer Institute and Harvard Medical School, Harvard Medical School, Boston, MA

[9]Department of Neurosurgery, Memorial Sloan-Kettering Cancer Center, New York, NY

[10]Department of Neurosurgery, Weill-Cornell Medical College, New York, NY

Abstract

Glioblastoma (GBM) is a highly lethal brain tumor presenting as one of two subtypes with distinct clinical histories and molecular profiles. The primary GBM subtype presents acutely as high-grade disease that typically harbors *EGFR, Pten* and *Ink4a/Arf* mutations, and the secondary GBM subtype evolves from the slow progression of low-grade disease that classically possesses *PDGF* and *p53* events[1–3]. Here, we show that concomitant CNS-specific deletion of *p53* and *Pten* in the

[11]correspondence: ron_depinho@dfci.harvard.edu, 617-632-6086 (office), 617-632-6069 (fax).
[12]These authors contributed equally to this work.

mouse CNS generates a penetrant acute-onset high-grade malignant glioma phenotype with striking clinical, pathological and molecular resemblance to primary GBM in humans. This genetic observation prompted *p53* and *Pten* mutational analysis in human primary GBM, demonstrating unexpectedly frequent inactivating mutations of *p53* as well the expected *Pten* mutations. Integrated transcriptomic profiling, in silico promoter analysis and functional studies of murine neural stem cells (NSCs) established that dual, but not singular, inactivation of *p53* and *Pten* promotes an undifferentiated state with high renewal potential and drives elevated c-Myc levels and its associated signature. Functional studies validated increased c-Myc activity as a potent contributor to the impaired differentiation and enhanced renewal of *p53-Pten* null NSCs as well as tumor neurospheres (TNSs) derived from this model. c-Myc also serves to maintain robust tumorigenic potential of *p53-Pten* null TNSs. These murine modeling studies, together with confirmatory transcriptomic/promoter studies in human primary GBM, validate a pathogenetic role of a common tumor suppressor mutation profile in human primary GBM and establish c-Myc as a key target for cooperative actions of p53 and Pten in the regulation of normal and malignant stem/progenitor cell differentiation, self-renewal and tumorigenic potential.

High-grade malignant glioma, the most common intrinsic brain tumor, is uniformly fatal despite maximum treatment[3]. A wealth of molecular genetic studies have established central roles of the RTK-PI3K-PTEN, ARF-MDM2-p53, and INK4a-RB pathways in gliomagenesis[3, 4]. To explore the role of p53 and Pten in glioma, we utilized the *hGFAP-Cre* transgene[5, 6] to delete *p53* alone or in combination with *Pten* in all CNS lineages using conditional *p53*[7] and *Pten* alleles (Supplementary Fig. 1, 2a-c). Since broad CNS deletion of *Pten* results in lethal hydrocephalus in early postnatal life (data not shown), modeling efforts henceforth emphasized the *Pten^{lox/+}* genotype.

Clinically, between ages 15 to 40 weeks, 42/57 (73%) of *hGFAP-Cre+;P53^{lox/lox};Pten^{lox/+}* mice presented with acute-onset neurological symptoms – seizure, ataxia, and/or paralysis (Fig. 1a). Histopathologically, all 42 neurologically symptomatic mice harbored malignant gliomas that, based on WHO criteria[8], were classified as anaplastic astrocytomas (WHO III, n=28, 66%) or GBM (WHO IV, n=14, 34%) (Fig. 1b) with classical features of pseudopalisading necrosis, marked cellular pleomorphism, and highly infiltrative spread including perineuronal and perivascular satellitosis as well as subpial spread in the cerebral cortex (Supplementary Fig. 3a). Occasional tumors exhibited abnormal vessels suggestive of microvascular proliferation. All tumors exhibited increased mitoses (Ki67 staining) and expression of classical human glioma markers, GFAP and Nestin (Fig. 1c). Necropsy of 15 neurologically asymptomatic mice showed no cases of incipient low-grade glioma disease but rather 8 with high-grade pathology including very small lesions with anaplastic features of nuclear atypia, multinucleated tumor cells, and/or high cellularity (Supplementary Fig. 3b). For the remaining genotypes, 4/23 *hGFAP-Cre;P53^{lox/lox}* mice developed anaplastic astrocytoma (WHO III); whereas 19/23 *hGFAP-Cre;P53^{lox/lox}*, 12/12 *hGFAP-Cre;P53^{lox/+};Pten^{lox/+}*, and 10/10 *hGFAP-Cre;P53^{lox/+}*) had no CNS pathology and developed only non-CNS tumors (data not shown).

Historically, *p53* inactivation has been considered a classical lesion in low-grade astrocytomas and secondary GBM, but infrequent in primary GBM[1, 9]. The remarkable

clinical and histological resemblance of this model to the primary GBM subtype in humans prompted *p53* and *Pten* re-sequencing in human primary GBM. Of 35 clinically annotated human primary GBM samples, 10/35 (29%) tumors registered prototypical *p53* mutations and 14/35 (40%) tumors possessed *Pten* missense mutations, insertions, deletions, or splicing mutations (Supplementary Table 1). Moreover, 6/10 tumors with p53 mutations harbored concomitant *Pten* mutations or homozygous deletion. Encouragingly, our mutational data agrees with The Cancer Genome Atlas data reporting *p53* and *Pten* as the two most commonly mutated tumor suppressor genes (http://tcga-data.nci.nih.gov/tcga/findArchives.htm). These results, together with recent population-based studies[10, 11], indicate that *p53* is a key tumor suppressor for both GBM subtypes.

Consistent with frequent *Pten* LOH (60–70%) in human high-grade glioma[3], 16/16 mouse high-grade glimoas showed no Pten expression in tumor cells but robust signal in surrounding non-malignant cells and intratumoral vessels (Fig. 2a). PCR geneotyping indicated that 6/7 tested tumors sustained loss of the wild-type *Pten* allele (Fig. 2b). The *Pten* reduction to homozygosity, and documented Cre-mediated deletion of both *p53* floxed alleles indicate that inactivation of both genes is required for gliomagenesis. Loss of Pten expression correlated with activation of key PI3K signaling surrogates, AKT and S6-Kinase (Fig. 2c). In accordance with human high-grade disease, 8/8 malignant murine gliomas expressed high VEGF levels relative to normal brain tissue (Fig. 2c). Multi-RTK co-activation in human primary GBM[12] was also evident in the murine tumors with robust PDGFRα expression overlapping with strong regional activation of EGFR (Supplementary Fig. 4a-d)

A classical feature of human high-grade malignant glioma is a significant degree of inter- and intra-tumoral morphological and lineage heterogeneity, hence the moniker glioblastoma 'mutliforme'. This characteristic plasticity was evident in the *hGFAP-Cre;P53^lox/lox^;Pten^lox/+^* gliomas wherein occasional tumors (5/50) presented with both astrocytic and oligodendroglial histopathological features (Supplementary Fig. 5). The basis for morphological variability is not known and may relate, among many possibilities, to acquisition of an immature developmental state with multipotency and/or differentiative plasticity. Consistent with this notion, all murine tumors express stem or lineage progenitor markers including Nestin, GFAP, and Olig2 similar to human glioma profiles[13], but negative for mature neuronal and oligodendrocyte markers, NeuN and MBP (Supplementary Fig. 6a-b). This stem/progenitor marker profile is in accord with the ability of all murine tumors tested to readily generate tumor neurospheres (TNS) with (i) strong tumor-initiating potential with secondary tumors faithfully retaining the primary tumor's histological features (Supplementary Fig. 7) (ii) robust NSC marker Nestin expression, and (iii) limited capacity to differentiate into astrocytic and neuronal lineages upon exposure to differentiation agents (Fig. 2d). As NSC/progenitor cells have been proposed to be the preferred cell-of-origin for GBM[6], the immature marker profile and varied morphological presentation of our murine tumors prompted us to posit that *Pten* and *p53* deficiencies might contribute to gliomagenesis by affecting NSC self-renewal and differentiation potential.

To explore this hypothesis, we characterized primary murine E13.5 NSC cultures singly or doubly null for *p53* and *Pten*. Compared to *Pten* or *p53* null NSCs which show only

modestly increased proliferation and self-renewal reflected by neurosphere formation capacity[14–16], NSCs null for *p53* and *Pten* exhibited significant proliferation and self-renewal activity (Fig. 3a; Supplementary Fig. 8a). This impact on NSC renewal, coupled with the aforementioned varied tumor histology, suggest that combined *p53* and *Pten* loss might cooperate in tumorigenesis by impairing NSC differentiation potential. When NSCs were continuously cultured in NSC medium, all gentoypes showed similar robust expression of NSC/progenitor markers (Nestin) and minimal expression of differentiated lineage markers (Supplementary Fig. 8b). Upon exposure to differentiation-inducing medium, wild-type and single-null NSC cultures differentiated into GFAP-positive astrocytes, Tuj1-positive neurons, or O4-positive oligodendrocytes. In contrast, NSCs null for both *p53* and *Pten* failed to respond to these differentiation cues and retained stem cell-like morphology and lineage marker (Nestin) expression (Fig. 3b; Supplementary Fig. 9a). Similar differentiation defect and abnormal self-renewal potential were also observed in adult NSCs that were deleted for *Pten* and *p53* postnatally (Supplementary Fig. 9b, c). The contribution of *Pten* deficiency in maintaining impaired differentiation was further verfied by the ability of the AKT inhibitor, Triciribine[17], to enable differentiation of *Pten/p53* null NSCs (Supplementary Fig. 10a, b).

To understand the molecular basis of impaired differentiation capacity, we performed transcriptome comparisons of *p53*-null and *p53/Pten* double-null murine NSCs at 1 day post exposure to the differentiation inducer. Among the 410 genes exhibiting significant differential expression (Supplementary Table 2), promoter analysis identified E2F and MYC motifs as two of the most enriched promoter binding elements (BE) (1.7x and 1.4x, respectively; $P < 10^{-4}$). Remarkably, promoter analysis using 69 pre-treatment human primary GBM cases in the TCGA database showed strong enrichment of Myc binding elements – 10 *p53/Pten* mutant tumors versus the 59 remaining tumors (1.40x, p=2.20x10^{-3}) or versus the 12 *p53* only mutant tumors (1.46x, p=1.54x10^{-3}).

c-MYC is well-known for its roles in cell cycle progression and apoptosis[18] as well as stem cell self-renewal and differentiation during development and oncogenic processes[19–22]. It is also notable that both p53 and Pten/PI3K pathways can directly regulate c-Myc with p53 repressing *c-MYC* transcription through direct binding to *c-MYC* promoter[23], while downstream PI3K pathway arms can modulate c-MYC translation and protein degradation[24, 25]. In agreement, c-Myc protein levels were substantially increased in the murine double-null NSCs, but only marginally elevated in single *p53*-null or *Pten*-null NSCs when compared to wild-type controls (Fig. 3c), raising the possibility that p53 and Pten cooperate to regulate c-Myc levels which in turn could control NSC self-renewal and differentiation.

To test this hypothesis, we examined the impact of c-Myc knockdown on murine *p53/Pten*-null NSC differentiation potential and observed that c-Myc shRNAs (#2 and #3), which reduced c-Myc levels to those in *p53*-null NSCs, largely restored their differentiation capacity (Fig. 3d; Supplementary Fig. 11a). Conversely, enforced c-Myc expression in p53-null NSCs repressed their differentiation and enabled retention of stem/progenitor marker expression (Nestin and Sox2) (Supplementary Fig. 11b), indicating that concomitant loss of p53 and Pten elevates c-MYC activity to impede NSC differentiation capacity.

The strong pleiotropic activities attributed to c-MYC demands tight control of its expression to avoid development of diverse human malignancies, including gliomas[21, 26]. Our finding that concomitant loss of p53 and Pten compromised NSC differentiation capacity via elevated c-Myc levels prompted further assessment of its relevance in the so-called 'brain cancer stem cells' in our model. Using murine TNSs which are enriched for such tumor initiating cells (TICs), AKT inhibitor treatment strongly reduced c-MYC protein and promoted differentiation (Fig. 4a, b; Supplementary Fig. 12a). Correspondingly, c-Myc knockdown in TNS cells not only markedly reduced their proliferation and self-renewal capacity (Fig. 4c; Supplementary Fig. 12b, c), but also strongly sensitized them to differentiation induction (Fig. 4d; Supplementary Fig. 12d). Importantly, while 10/10 intracranial injections of vector-transduced murine TNSs resulted in lethal infiltrating gliomas within 1 month, 9/10 mice injected with c-Myc knockdown TNSs survived for more than 3 months (Fig. 4e). Thus, c-MYC plays a key role in the maintenance of impaired differentiation and potent tumorigenic potential of TNSs inactivated for *p53* and *Pten* (Supplementary Fig. 13).

The identification of TICs with stem-like properties in diverse human cancers including GBM represents an important conceptual advance in cancer biology with therapeutic implications[27, 28]. These TICs appear to constitute a reservoir of self-sustaining cells with potent tumorigenic potential. However, unlike normal NSCs which readily differentiate along a developmental hierarchy into lineage-restricted differentiated progenies, TNSs derived from *p53/Pten*-null malignant gliomas show resistance towards differentiation cues. The diminished tumorigenicity of these TICs upon restoration of differentiation potential, along with recent reports supporting pro-differentiation as a potential strategy to inhibit GBM-derived TICs[29, 30], encourages the identification and testing of agents targeting these differentiation pathways including c-Myc in the treatment of primary GBM in humans.

Full Methods

Mice

P53^L and *hGFAP-Cre* mice have been described previously[5, 7]. *Pten^L* mice were generated using a standard knock-in approach in which *Pten* exon 5 is flanked by loxP sites (details on targeting construct and procedures are available upon request). Mice were interbred and maintained on FvB/C57Bl6 hybrid background in pathogen-free conditions at Dana-Farber Cancer Institute, monitored for signs of ill-health every other day, and euthanized and necropsied when moribund. All manipulations were performed with IACUC approval.

Histology and Immunohistochemistry

At time of sacrifice, mice were perfused with 4% paraformaldehyde (PFA), and brains were dissected, followed by overnight post-fixation in 4% PFA at 4°C. Serial sections were prepared at 5 μm for paraffin sections or 10 μm for cryostat sections with every tenth slide stained by haematoxylin and eosin (DF/HCC Research Pathology Cores). Tumor grading was determined by K.L.L and H.Z. based upon the WHO grading system for malignant astrocytoma[8]. Immunohistochemical and immunofluorescence analyses were performed as described[31]. The PDGFRα/pEGFR double immunohistochemical staining was performed

using DakoCytomation EnVision doublestain system (K1395, Dako) following manufacturer instructions. The primary antibodies used were: Ki67 (VP-RM04, Vector), GFAP (Z0334, DAKO), GFAP (556330, BD Pharmingen), Nestin (MAB353, Chemicon; specifically for mouse), Nestin (MAB5326, Chemicon; specifically for human), Pten (9559, Cell Signaling), Phospho-Akt^{Ser473} (3787, Cell Signaling), phospho-S6 ribosomal protein (2215, Cell Signaling), Cyclin D1 (18-0220, ZYMED), VEGF (sc-152, Santa Cruz), PDGFRα (3174, Cell Signaling), Phospho-PDGFRa^{Y754} (sc-12911, Santa Cruz), EGFR (IHC-00005, Bethyl), Phospho-EGFR^{Y1068} (ab40815, Abcam), Phospho-EGFR^{Y1173} (sc-12351, Santa Cruz), Olig-2 (AB9610, Chemicon), TUJ-1 (MMS-435P, Covance), O4 (MAB1326, R&D), NeuN (MAB377, Millipore), MBP (ab7349, Abcam), c-Myc (ABcam, ab39688), and Cre (69050-3, Novagen). Images were captured using a Leica DM1400B microsystem and Leica FW4000 version 1.2.1.

Cell culture

Primary NSCs were isolated from the brain subventricular zone (SVZ) of E13.5 embryos or 1 month old mice with the indicated genotype as previously described[31, 32]. NSCs were maintained in NSC proliferation media (05702, StemCell) supplemented with 20 ng/mL EGF (E4127, Sigma) and 10ng/mL bFGF (F0291, Sigma). To generate primary TNS cells, tumor samples from freshly dissected mouse brains were subjected to mechanical and enzymatic dissociation. Single-cell suspensions were cultured in NSC proliferation media. Tumor spheres formed were then disaggregated and used for indicated assays. NSC differentiation assays were carried out by plating the indicated cells in culture wells on coverslips pre-coated with 15 μg/mL poly-L-ornithine (P3655, Sigma) and 1 μg/mL fibronectin (F1141, Sigma); the cells were incubated in neurobasal medium supplemented with 1% FBS for 7–10 days, and the differentiation capacities examined under either light or fluorescence microscope (Nikon). For TNS cell differentiation, cells were incubated in differentiation media with varying doses of triciribine (BioMol) or vehicle (DMSO, Sigma). Knockdown of mouse c-Myc was performed by infecting the indicated cells with lentivirus containing shMyc constructs (provided by Dr. William Hahn, Dana Farber Cancer Institute). The shRNA constructs shMyc #1, #2 and #3 correspond to clone ID#s TRCN000000 54856, 42517 and 42513, respectively (The DFCI-Broad RNAi Consortium, commercially available from Sigma-Aldrich).

Western, cell growth and self-renewal assays

Western blot assays were performed as previously described[31] with antibodies against c-Myc (sc-42, Santa Cruz), Phospho-AKT^{Ser473} (9271, Cell signaling), Pten (9569, Cell Signaling) and Actin (sc-1615, Santa Cruz). For in vitro cell growth assays, NSCs or TNS cells (10,000) were plated in triplicate in 96-well format and incubated in NSC proliferation media for 5 days, and growth was quantified using Luminescence ATP detection assay system (PerkinElmer). Self-renewal capacity was measured by plating 1,000 cells/well (6-well plate) in NSC proliferation media containing EGF/bFGF with 0.3% agarose (A9049, Sigma). The number of neurospheres or tumor neurospheres that formed subsequently per well was quantified after 10–14 days and relative sphere formation was plotted versus indicated control. Three replicates were performed for each. All experiments were conducted at cell passage <5.

Orthotopic transplants

Female SCID (Charles River) aged 6–8 weeks were anesthetized and placed into stereotactic apparatus equipped with a Z axis (Stoelting). A small hole was bored in the skull 0.5 mm anterior and 3.0 mm lateral to the Bregma using a dental drill. 2×10^4 cells in Hanks Buffered Salt Solution was injected into the right caudate nucleus 3 mm below the surface of the brain using a 10 μl Hamilton syringe with an unbeveled 30 gauge needle. The scalp was closed using a 9 mm Autoclip Applier. Animals were followed daily for development of neurological deficits.

Mutation screening

Frozen tumor specimens were obtained from the Memorial Sloan Kettering Cancer Center tumor bank. Genomic DNA was prepared from frozen primary GBM tumour samples using the Qiagen genomic purification kit. Coding exons were PCR amplified and sequenced using standard protocols at the Harvard Partners Center for Genetics and Genomics as previously described[33]. All known single-nucleotide polymorphisms and synonymous mutations were removed from the analysis in the current study. This study was approved by the Institutional Review Board of the hospital.

Microarray analysis

Early passage wild-type and indicated mutant NSCs were incubated with NSC proliferation media or differentiation media for 18 hours. RNA was isolated using Trizol (Invitrogen) and the RNeasy mini kit (Qiagen). Gene expression profiling was performed utilizing the Affymetrix 430 2.0 chips at DFCI Microarray core facility.

Promoter Analysis

Gene expressions were modeled using dChip software[34]. Sets of genes differentially expressed pre- and post- differentiation induction were generated using the SAM statistic[35], with a cutoff of +/− 2.0. Promoter analysis on both these gene sets used the CisGenome software (http://biogibbs.stanford.edu/~jihk/CisGenome/index.htm) to scan the 8 kb upstream to 2kb downstream regions of these genes for the ~550 motifs in the TRANSFAC 12.1 database. Enrichment was measured against control regions at a comparable distance from the transcription start sites of random genes.

Statistical analysis

Tumor-free survivals were analyzed using Graphpad Prism4. Statistical analyses were performed using nonparametric Mann–Whitney test. Significance of enrichment in the promoter analysis was computed based on Poisson distribution with Bonferroni correction. Comparisons of cell growth, self-renewal and differentiation were performed using the unpaired Student's t-test. For all experiments with error bars, standard deviation was calculated to indicate the variation within each experiment and data, and values represent mean ± s.d.

Supplementary Material

Refer to Web version on PubMed Central for supplementary material.

Acknowledgments

References

1. Kleihues P, Ohgaki H. Primary and secondary glioblastomas: from concept to clinical diagnosis. Neuro Oncol. 1999; 1:44–51. [PubMed: 11550301]

2. Zhu Y, Parada LF. The molecular and genetic basis of neurological tumours. Nat Rev Cancer. 2002; 2:616–626. [PubMed: 12154354]

3. Furnari FB, et al. Malignant astrocytic glioma: genetics, biology, and paths to treatment. Genes Dev. 2007; 21:2683–2710. [PubMed: 17974913]

4. Wiedemeyer R, et al. Feedback circuit among INK4 tumor suppressors constrains human glioblastoma development. Cancer Cell. 2008; 13:355–364. [PubMed: 18394558]

5. Zhuo L, et al. hGFAP-cre transgenic mice for manipulation of glial and neuronal function in vivo. Genesis. 2001; 31:85–94. [PubMed: 11668683]

6. Zhu Y, et al. Early inactivation of p53 tumor suppressor gene cooperating with NF1 loss induces malignant astrocytoma. Cancer Cell. 2005; 8:119–130. [PubMed: 16098465]

7. Jonkers J, et al. Synergistic tumor suppressor activity of BRCA2 and p53 in a conditional mouse model for breast cancer. Nat Genet. 2001; 29:418–425. [PubMed: 11694875]

8. Louis, DN.; Ohgaki, H.; Wiestler, OD.; Cavenee, WK. WHO Classification of Tumours of the Central Nervous System, Fourth Edition. Louis, DN.; Ohgaki, H.; Wiestler, OD.; Cavenee, WK., editors. Lyon, France: World Health Organization; 2007.

9. Watanabe K, et al. Overexpression of the EGF receptor and p53 mutations are mutually exclusive in the evolution of primary and secondary glioblastomas. Brain Pathol. 1996; 6:217–223. discussion 23-4. [PubMed: 8864278]

10. Ohgaki H, et al. Genetic pathways to glioblastoma: a population-based study. Cancer Res. 2004; 64:6892–6899. [PubMed: 15466178]

11. Fukushima T, et al. Genetic alterations in primary glioblastomas in Japan. J Neuropathol Exp Neurol. 2006; 65:12–18. [PubMed: 16410744]

12. Stommel JM, et al. Coactivation of receptor tyrosine kinases affects the response of tumor cells to targeted therapies. Science. 2007; 318:287–290. [PubMed: 17872411]

13. Ligon KL, et al. Olig2-regulated lineage-restricted pathway controls replication competence in neural stem cells and malignant glioma. Neuron. 2007; 53:503–517. [PubMed: 17296553]

14. Groszer M, et al. PTEN negatively regulates neural stem cell self-renewal by modulating G0-G1 cell cycle entry. Proc Natl Acad Sci U S A. 2006; 103:111–116. [PubMed: 16373498]

15. GilPerotin S, et al. Loss of p53 induces changes in the behavior of subventricular zone cells: implication for the genesis of glial tumors. J Neurosci. 2006; 26:1107–1116. [PubMed: 16436596]

16. Meletis K, et al. p53 suppresses the self-renewal of adult neural stem cells. Development. 2006; 133:363–369. [PubMed: 16368933]

17. Yang L, et al. Akt/protein kinase B signaling inhibitor-2, a selective small molecule inhibitor of Akt signaling with antitumor activity in cancer cells overexpressing Akt. Cancer Res. 2004; 64:4394–4399. [PubMed: 15231645]

18. Patel JH, Loboda AP, Showe MK, Showe LC, McMahon SB. Analysis of genomic targets reveals complex functions of MYC. Nat Rev Cancer. 2004; 4:562–568. [PubMed: 15229481]

19. Cartwright P, et al. LIF/STAT3 controls ES cell self-renewal and pluripotency by a Myc-dependent mechanism. Development. 2005; 132:885–896. [PubMed: 15673569]

20. Takahashi K, Yamanaka S. Induction of pluripotent stem cells from mouse embryonic and adult fibroblast cultures by defined factors. Cell. 2006; 126:663–676. [PubMed: 16904174]

21. Ben-Porath I, et al. An embryonic stem cell-like gene expression signature in poorly differentiated aggressive human tumors. Nat Genet. 2008; 40:499–507. [PubMed: 18443585]

22. Wong DJ, et al. Module map of stem cell genes guides creation of epithelial cancer stem cells. Cell Stem Cell. 2008; 2:333–344. [PubMed: 18397753]

23. Ho JS, Ma W, Mao DY, Benchimol S. p53-Dependent transcriptional repression of c-myc is required for G1 cell cycle arrest. Mol Cell Biol. 2005; 25:7423–7431. [PubMed: 16107691]

24. Gera JF, et al. AKT activity determines sensitivity to mammalian target of rapamycin (mTOR) inhibitors by regulating cyclin D1 and c-myc expression. J Biol Chem. 2004; 279:2737–2746. [PubMed: 14576155]

25. Sears R, et al. Multiple Ras-dependent phosphorylation pathways regulate Myc protein stability. Genes Dev. 2000; 14:2501–2514. [PubMed: 11018017]

26. Bredel M, et al. Functional network analysis reveals extended gliomagenesis pathway maps and three novel MYC-interacting genes in human gliomas. Cancer Res. 2005; 65:8679–8689. [PubMed: 16204036]

27. Clarke MF, et al. Cancer stem cells--perspectives on current status and future directions: AACR Workshop on cancer stem cells. Cancer Res. 2006; 66:9339–9344. [PubMed: 16990346]

28. Lobo NA, Shimono Y, Qian D, Clarke MF. The biology of cancer stem cells. Annu Rev Cell Dev Biol. 2007; 23:675–699. [PubMed: 17645413]

29. Piccirillo SG, et al. Bone morphogenetic proteins inhibit the tumorigenic potential of human brain tumour-initiating cells. Nature. 2006; 444:761–765. [PubMed: 17151667]

30. Lee J, et al. Epigenetic-mediated dysfunction of the bone morphogenetic protein pathway inhibits differentiation of glioblastoma-initiating cells. Cancer Cell. 2008; 13:69–80. [PubMed: 18167341]

31. Bachoo RM, et al. Epidermal growth factor receptor and Ink4a/Arf: convergent mechanisms governing terminal differentiation and transformation along the neural stem cell to astrocyte axis. Cancer Cell. 2002; 1:269–277. [PubMed: 12086863]

32. Rietze RL, Reynolds BA. Neural stem cell isolation and characterization. Methods Enzymol. 2006; 419:3–23. [PubMed: 17141049]

33. Maser RS, et al. Chromosomally unstable mouse tumours have genomic alterations similar to diverse human cancers. Nature. 2007; 447:966–971. [PubMed: 17515920]

34. Li C, Wong WH. Model-based analysis of oligonucleotide arrays: expression index computation and outlier detection. Proc Natl Acad Sci U S A. 2001; 98:31–36. [PubMed: 11134512]

35. Tusher VG, Tibshirani R, Chu G. Significance analysis of microarrays applied to the ionizing radiation response. Proc Natl Acad Sci U S A. 2001; 98:5116–5121. [PubMed: 11309499]
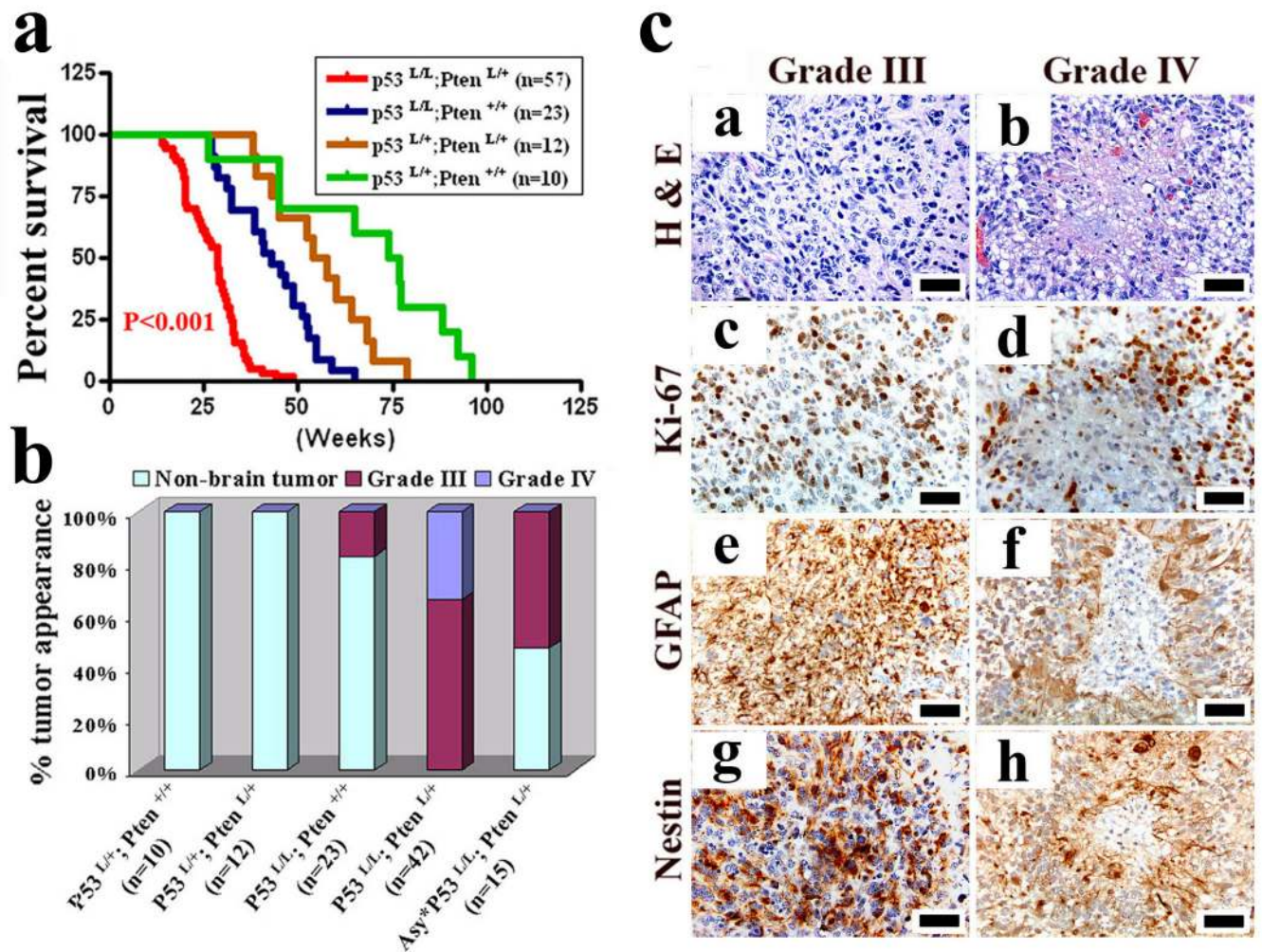
Figure 1. *p53* and *Pten* inactivation cooperate to induce high-grade malignant gliomas

a, Kaplan-Meier tumor-free survival curves for mice of indicated genotypes as a function of weeks.

b, Graph shows frequency and grade of gliomas *vs.* non-CNS malignancies observed in end-stage of indicated mice from **a**. *Asy** indicates neurological asymptomatic *hGFAP-Cre;P53^{lox/lox};Pten^{lox/+}* mice (n=15) sacrificed for non-CNS malignancies.

c, H&E histology and immunohistochemical staining of sections of WHO grade III and grade IV malignant gliomas from *hGFAP-Cre;P53^{lox/lox};Pten^{lox/+}* mice with antibodies against Ki67, GFAP, and Nestin. Scale bar, 50 μm.
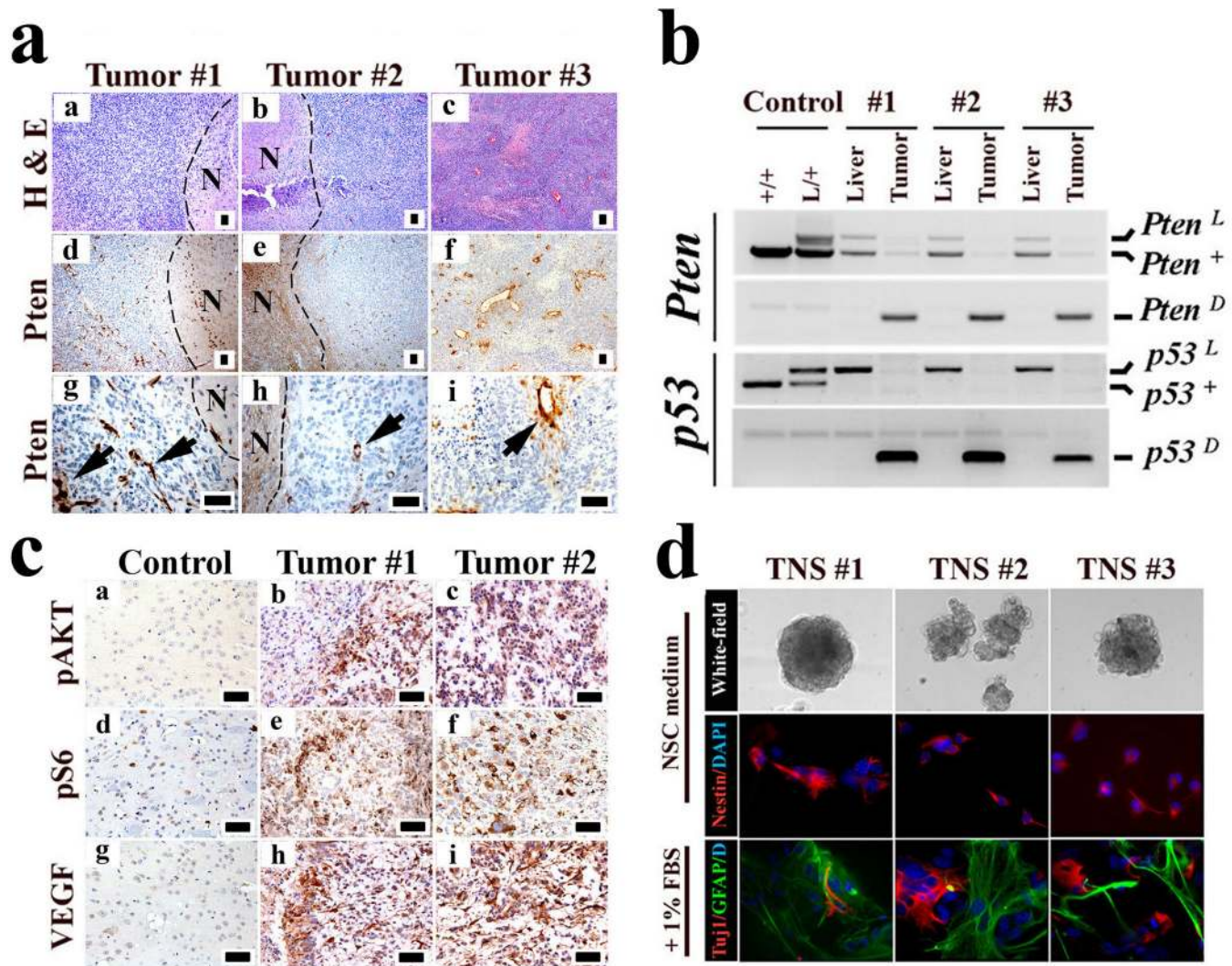
Figure 2. *hGFAP-Cre;P53^{lox/lox};Pten^{lox/+}* **gliomas mirror key features of human malignant gliomas**

a, Pten expression is completely extinguished in tumor cells. Sections of three independent malignant gliomas were stained with H&E, and an anti-Pten antibody. Note "N" indicates the adjacent normal regions of the tumor cells; the arrows point to Pten-positive vascular cells embedded in the tumor.

b, Wild-type *Pten* allele is lost in glioma cells. Genomic DNA isolated from liver tissues and brain tumor cells were subjected to PCR-based assays for genotyping *Pten* and *p53* alleles. Note "+" designates the *Pten* wild-type allele; "*L*" the conditional allele; and "*D*" the inactivated form of the conditional allele after Cre-mediated recombination.

c, Immunohistochemical staining of mouse normal brain or glioma sections with antibodies against activated p-AKT, p-S6 kinase, and VEGF.

d, TNS lines isolated from independent malignant gliomas were cultured in NSC medium or differentiation medium and immuno-stained for Nestin, GFAP and Tuj1 as indicated. Scale bar, 50 μm.
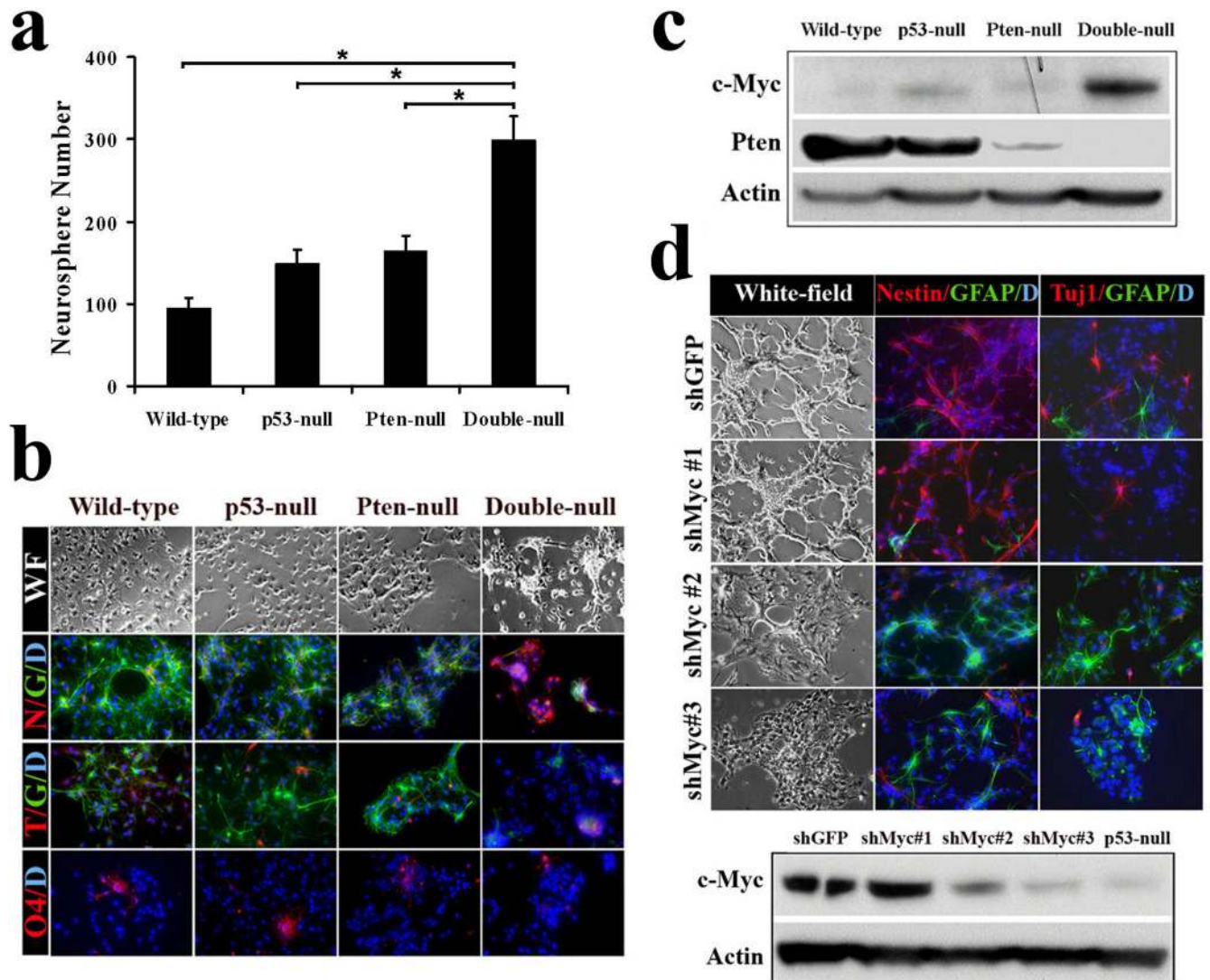
Figure 3. *p53* **and** *Pten* **coordinately regulate c-Myc protein level as well as NSC self-renewal and differentiation**

a, The number of neurospheres formed by *p53/Pten* double-null NSCs in culture is significantly increased as compared to wild-type or singly null NSCs (*$P < 0.001$; n=3). Values represent mean ± s.d. from three experiments.

b, The multi-lineage differentiation potential was impaired in double-null NSCs. Note "WF" designates for white-field; N for Nestin (red); G for GFAP (green); T for Tuj-1 (red); O4 (red); D for DAPI (blue).

c, Combined inactivation of *p53* and *Pten* in NSCs stimulates c-Myc protein expression.

d, Knockdown of c-Myc expression restores *p53/Pten* double-null NSCs differentiation capacity. Lower panel, western blot of double-null NSC c-Myc protein expression after infected with indicated lenti-shRNA. Note c-Myc expression in shMyc #2 and #3 infected double-null cells is comparable to that in *p53*-null cells, and shMyc #1 as a control shows no knockdown.
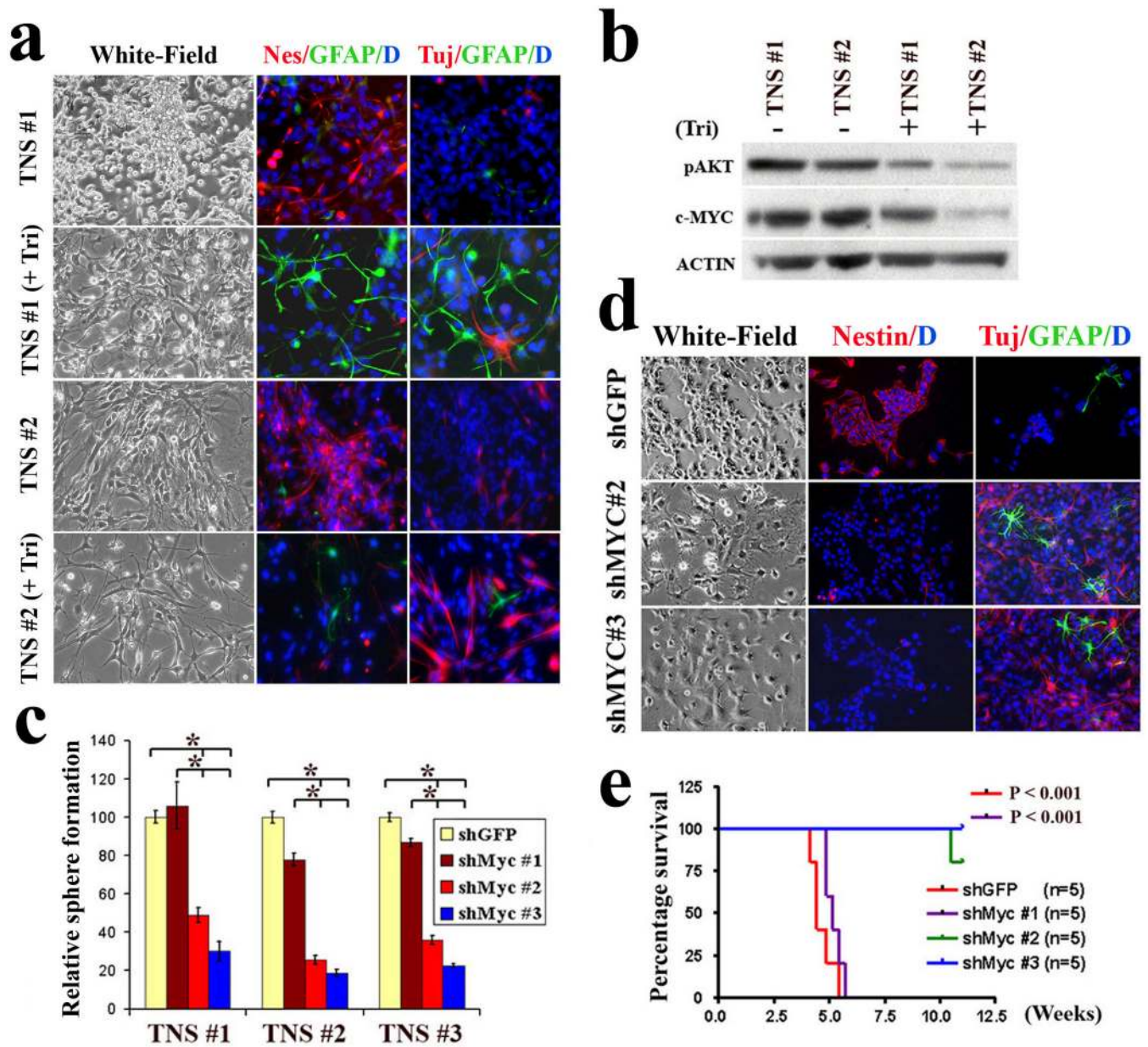
Figure 4. Attenuated c-Myc expression restores *hGFAP-Cre;P53$^{lox/lox}$;Pten$^{lox/+}$* TNS differentiation potential and reduces tumorigenic potential

a, Inhibition of the AKT pathway by triciribine induces TNS cell differentiation. Two independent TNS lines were cultured in 1% FBS in the absence or presence of triciribine (5 μM) for 7 days before being subjected to immuno-staining with antibodies against Nestin (red), GFAP (Green) and Tuj1 (red).

b, Inhibition of the AKT pathway in TNS cells with triciribine attenuates their cellular c-Myc expression.

c, Knockdown of c-Myc expression in TNS cells reduces their self-renewal potential assessed by sphere formation (*$P < 0.001$, n=3). Values represent mean ± s.d. from three experiments.

d, ShRNA-mediated reduction of c-Myc expression in TNS cells sensitizes cells to differentiation stimuli. Cells infected with control and indicated shRNA were incubated with differentiation medium before subjected to indicated lineage marker analysis.
e, ShRNA-mediated reduction of c-Myc expression represses TNS tumorigenic potency in orthotopically transplanted SCID mice.